Eur. J. Mineral.
2003, **15**, 977-989

Garnet-chloritoid-kyanite metapelites from the Raspas Complex (SW Ecuador): a key eclogite-facies assemblage

PIERCARLO GABRIELE[1,3,*], MICHEL BALLÈVRE[1], ETIENNE JAILLARD[2] and JEAN HERNANDEZ[3]

[1]Equipe Lithosphère, Géosciences Rennes (UMR CNRS 6118), Université de Rennes 1, F-35042 Rennes Cedex, France
[2]Institut pour la Recherche et le Développement - Laboratoire de Géologie des Chaînes Alpines, BP 53, F-38041 Grenoble Cedex 9, France
[3]Institut de Minéralogie et Géochimie, Université de Lausanne, BFSH2, CH-1015 Lausanne, Suisse

Abstract: The Raspas Complex (Ecuador) contains one of the few eclogitic bodies in the northern Andes. It consists of metaperidotites, eclogites, and metapelites. The latter display three assemblages: (i) garnet + chloritoid + kyanite, (ii) garnet + chloritoid and (iii) garnet + chlorite, in all cases with quartz and muscovite in addition. The growth of these assemblages was coeval with the main ductile deformation, and was followed by minor reequilibration (chlorite growth in garnet + chloritoid samples and chloritoid + quartz aggregates replacing garnet and kyanite in garnet + chloritoid + kyanite samples). Detailed microprobe analyses show increasing magnesian compositions for garnet (from core to rim) and chloritoid (inclusions within garnet compared to matrix grains) in kyanite-bearing samples. The above data are interpreted in the framework of the KFMASH system. Reaction progress along the divariant reaction Cld = Grt + Ky explains the change in chemistry of coexisting phases. The divariant Grt-Cld-Ky assemblage has a narrow stability field, and the P-T conditions are estimated at about 20 kbar, 550-600°C. Decompression, recorded by chloritoid-quartz pseudomorphs of garnet, probably occurred as temperature decreased.

Key words: eclogite-facies metamorphism; Ecuador; metapelite; Raspas Complex.

Mineral abbreviations are from Kretz (1983).

Introduction

Since the advent of plate tectonics, high-pressure metamorphic rocks have been recognised as an essential characteristic of convergent plate boundaries. Most blueschists and eclogites are derived from subduction of oceanic lithosphere, but relics of high-pressure to ultra-high-pressure parageneses in continentally-derived material have also proven the existence of continental subduction (*e.g.* Compagnoni *et al*., 1977; Chopin, 1984; Maruyama *et al*., 1996). The link between high-pressure metamorphism and lithospheric subduction results from the thermal structure of subduction zones, where low geothermal gradients prevail during convergence (*e.g.* Ernst, 1973; Peacock, 1996).

The Andean Range along the western side of South America is a typical example of an active margin, where the oceanic crust from the Pacific and Nazca plates is currently being subducted under the South American continent. A thickened crust has developed above the subduction zone as a result of magmatic underplating and/or accretion at various times of magmatic arcs and oceanic plateaux (Gansser, 1973; Feininger & Bristow, 1980; Aspden & McCourt, 1986; Mégard, 1987; Litherland *et al*., 1994). High-pressure rocks developed at some stage during the long-standing subduction history are sparsely represented along the Andean Range (see review in Maruyama *et al*., 1996). In the northern Andes three occurrences of high-pressure rocks have been found in Colombia (Orrego *et al*., 1980; Feininger, 1982a; de Souza *et al*., 1984) and one in Ecuador (Feininger, 1980).

This study aims at clarifying the P-T evolution of one of these occurrences, namely the Raspas Complex in southern Ecuador (Feininger, 1980). In particular, the purpose of this study is to document the reaction history and P-T conditions of well-preserved occurrences of garnet-chloritoid-kyanite metapelites. Because this paragenesis is a rare eclogite-facies assemblage, it can be considered as a key for the determination of high-pressure conditions in pelitic systems.

Geological setting

Ecuador can be divided into two main domains separated by a major suture zone striking N/NE-S/SW and

*E-mail: Piercarlo.Gabriele@univ-rennes1.fr

DOI: 10.1127/0935-1221/2003/0015-0977
0935-1221/03/0015-0977 $ 5.85

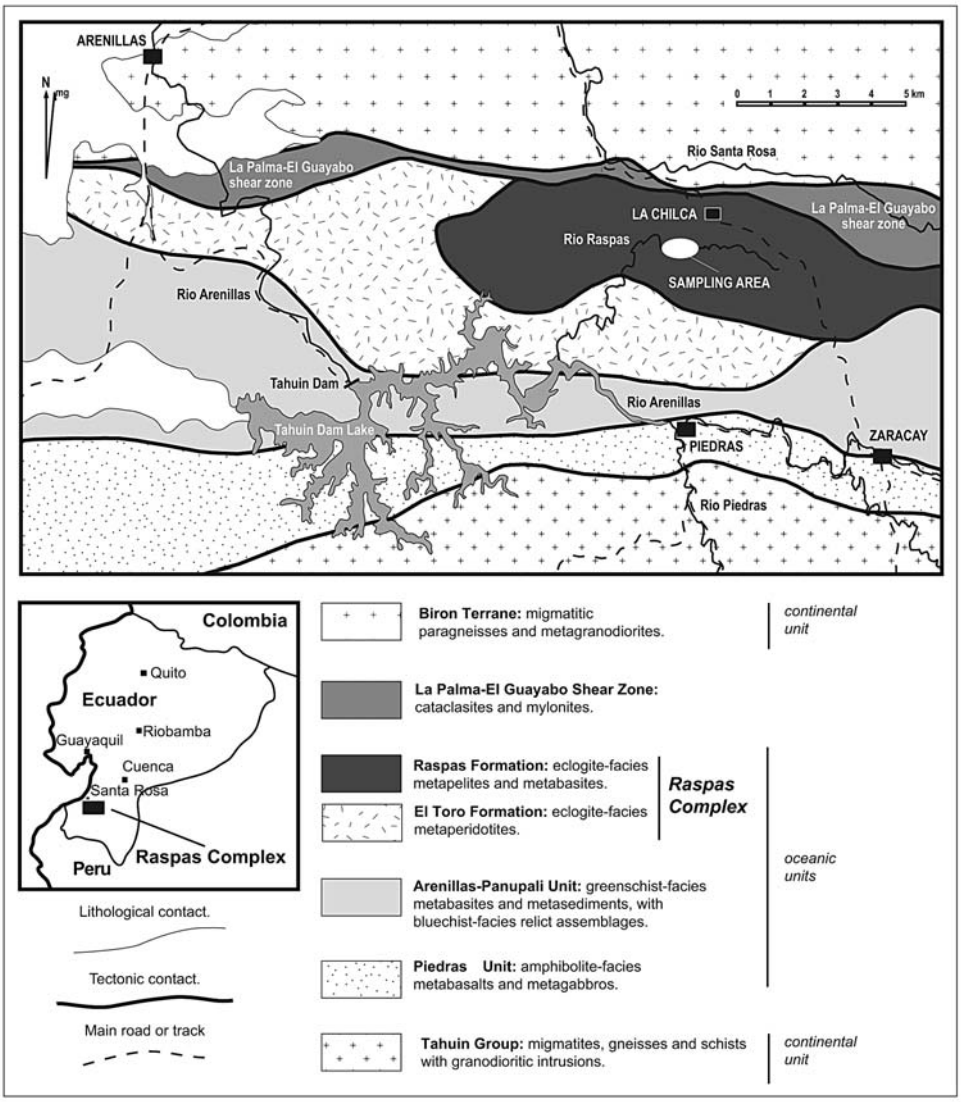

Fig. 1. Simplified tectonic map of the studied area, El Oro Province, southwestern Ecuador (Gabriele, 2002).

located between the eastern margin of the inter-Andean valley and the western foot of the Cordillera Real.

The eastern domain, of continental derivation, is composed of the Precambrian Amazon craton, covered by the Tertiary-Quaternary deposits of the Oriente Basin, and of a variety of metamorphic and magmatic rocks, Palaeozoic to Jurassic in age, forming the Cordillera Real. This domain was the active continental margin facing the subduction zone until the end of the Jurassic (*ca*. 140 Ma) (Aspden *et al*., 1987; 1995; Jaillard *et al*., 1990).

In the western domain, between 1°N and 3°S, most of the geological units of the Western Cordillera and Coastal Domain are magmatic bodies with an oceanic affinity, associated with different subduction-accretion events occurring since Early Cretaceous times (Gansser, 1973; Feininger & Bristow, 1980; Litherland *et al*., 1994; Jaillard *et al*., 1997; Reynaud *et al*., 1999; Spikings *et al*., 2001; Hughes & Pilatasig, 2002).

In the El Oro province of south-western Ecuador (between 3°S and 4°S; 79°30'W and 80°50'W), the Cordillera de Tahuin, a foothills range west of the Andes, forms the western shoulder of the South American continent. In this region, various metamorphic terranes (Feininger, 1982b) have been grouped together as the "El Oro Metamorphic Complex" (about 2,700 km^2) (Aspden *et al.*, 1995). These terranes can be interpreted (i) as independent allochtonous or parautochtonous bodies (Feininger, 1987), (ii) as large displaced blocks (*Amotape-Tahuin block* of Mourier *et al*., 1988), (iii) as a late Jurassic - early Cretaceous tectonic mélange representing part of an accretionary prism (Aspden *et al.*, 1995). The El Oro Metamorphic Complex is characterised by varied lithologies and assemblages, the metamorphic ages of which range from the Palaeozoic to the Cretaceous (Aspden *et al*., 1995). According to Aspden *et al*. (1995), this area is crosscut by several E-W-trending strike-slip faults that subdivide the El Oro Metamorphic Complex into smaller units.

One of these, the Raspas Complex, is bounded to the North by the La Palma - El Guayabo shear zone and to the South by a major tectonic contact (Fig. 1). The Raspas

Table 1. Mineral assemblages of the analysed samples. Abbreviations follow Kretz (1983), except W.M. (white mica).

Assemblage	Grt+Cld+Ky			Grt+Cld			Grt+Chl			
Sample	98RR11	97Ce5	97Ce6	98RR2	98RR12	97Ce4	98RR7	98RR10	97Ce2	97Ce3
Qtz	x	x	x	x	x	x	x	x	x	x
W.M.	x	x	x	x	x	x	x	x	x	x
Grt	(x)	(x)-x	(x)-x	(x)	(x)	(x)	x	x	x	x
Cld	II-IIIa-IIIb	I-II-IIIa-IIIb	II-IIIa-IIIb	II-IIIa-IIIb	II-IIIa-IIIb	II-IIIa-IIIb				
Chl				III	III		II	II	II	II
Ky	x	x	x							
Rt	x	x	x	x	x	x	x	x	x	x
Ttn								I		
Gr	x	x	x	x	x	x	x		x	x
Tur				x						
Ap								x		
Sulphides		x	x	x		x	x		x	
Microprobe analyses	+	+		+	+			+		+
Whole-rock chem. anal.	+	+	+	+	+				+	+

Abbreviations are after Kretz (1983); in addition W.M., white mica; (x),pseudomorphosed; I, inclusion in Grt; II, synkinematic; III, post-kinematic (IIIa : pseudomorph of Grt ; IIIb : porphyroblasts randomly oriented across the main schistosity).

Complex comprises two formations, namely the El Toro Formation, made of eclogite-facies metaperidotites, and the Raspas Formation, consisting of eclogites, garnet-amphibolites, blueschists and garnet-chloritoid micaschists (Feininger, 1978, 1980; Gabriele, 2002). Geochemical data show that the Raspas Complex is a composite fragment of oceanic lithosphere, the eclogite-facies mafic rocks presenting OPB-type affinities (Arculus *et al*., 1999; Bosch *et al.*, 2002). To the south of the Raspas Complex, the mafic rocks from the Arenillas-Panupali and Piedras Units show MORB-type affinities (Aspden *et al*., 1995; Bosch *et al.*, 2002; Gabriele, 2002). The Raspas Complex, in association with the Arenillas-Panupali and Piedras Units, represents a piece of oceanic lithosphere sandwiched between continentally-derived units, *i.e.* the Biron Terrane to the North, and the Tahuin Group to the South (Feininger, 1978 and 1987; Gabriele, 2002) (Fig. 1). K-Ar data on phengite (132 ± 5 Ma, Feininger, 1980) suggest a lowermost Cretaceous age for cooling of the high-pressure metamorphism.

Petrography

The studied pelitic schists have been sampled in the northern part of the Raspas Complex. The best outcrops are located in the Rio Raspas, where the trail from La Chilca village crosses the brook (Fig. 1, UTM-WGS84: 17 / 620500E-9602100N).

The metapelites (Table 1) are medium- to coarse-grained graphite-bearing schists, with conspicuous crystals of garnet up to 1 cm in diameter. Most garnet grains are blackish rather than reddish, either because they contain abundant graphite inclusions or because they are partially to wholly replaced by a fine-grained aggregate consisting of chloritoid and quartz.

Textural observations show an early, synkinematic, stage of mineral growth, followed by post-kinematic growth (Fig. 2). While syn-kinematic phengite clearly defines the main schistosity, the relation between graphite growth and deformation is more ambiguous. The graphite occurs mainly as an internal schistosity in garnet porphyroblasts (Fig. 3a) or as rootless isoclinal folds (in microlithons) having an axial plane sub-parallel to the main schistosity. This observation is consistent with the existence of several generations of structures (*e.g.* the graphite-bearing schistosity preserved within garnet or microlithons) developed before the main schistosity (*i.e.* the schistosity defined by shape-preferred orientation of phengite).

The white mica defines the main schistosity (*i.e.* the external schistosity) which corresponds in the field to the regional schistosity (Fig. 3). Idioblastic or sub-idioblastic phengite is usually concentrated in millimetre-thick layers alternating with quartz-rich, granoblastic layers. Some white mica aggregates are oblique to the main schistosity, and define microlithons which include rootless isoclinal folds defined by graphite-rich layers.

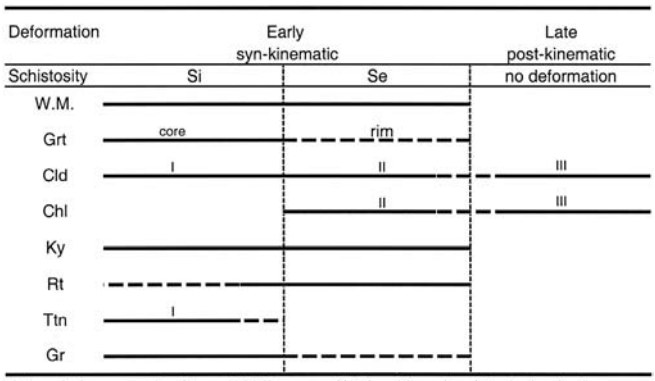

Abbreviations are after Kretz (1983), except W.M.: white mica. I, inclusion in Grt; II, synkinematic; III, post-kinematic. Si and Se refer to the internal (i.e. in Grt porphyroblasts) and external (i.e. in the matrix) schistosity. Ttn has been observed only in sample 98RR10.

Fig. 2. Timing of mineral growth and ductile deformation in the metapelites from the Raspas Complex.

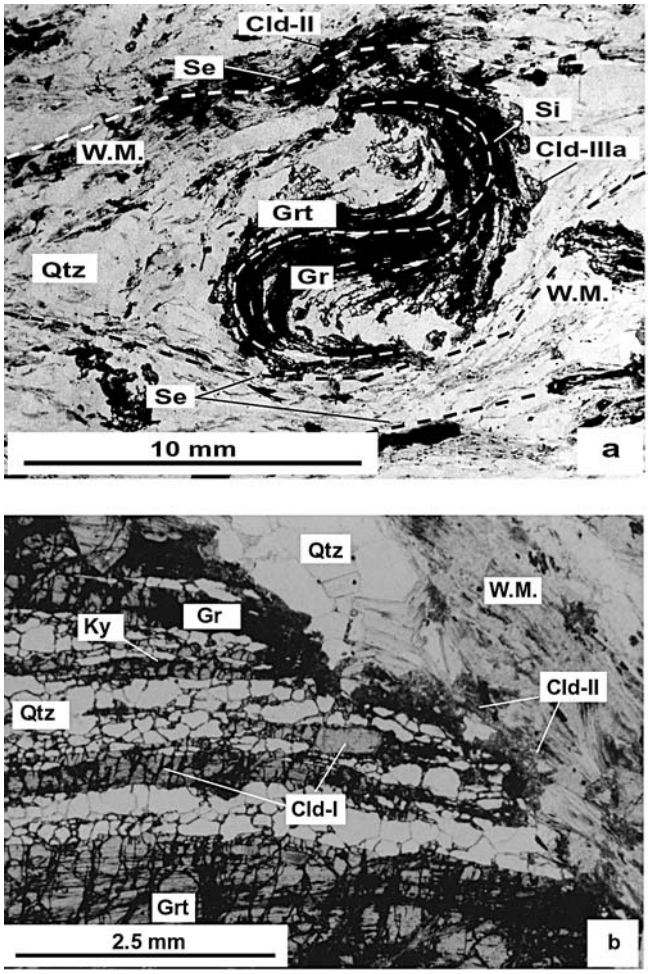

Fig. 3. Photomicrographs (plane-polarised light) showing the main textural features of the Raspas metapelites. (a): Garnet porphyroblast with aligned inclusions defining an internal schistosity (Si) (sample 98RR2) and showing rotation with respect to the external schistosity (Se). (b) Garnet poikiloblast showing alternating quartz-rich and quartz-poor layers, and inclusions of kyanite, chloritoid (Cld I) and graphite (sample 97Ce5).

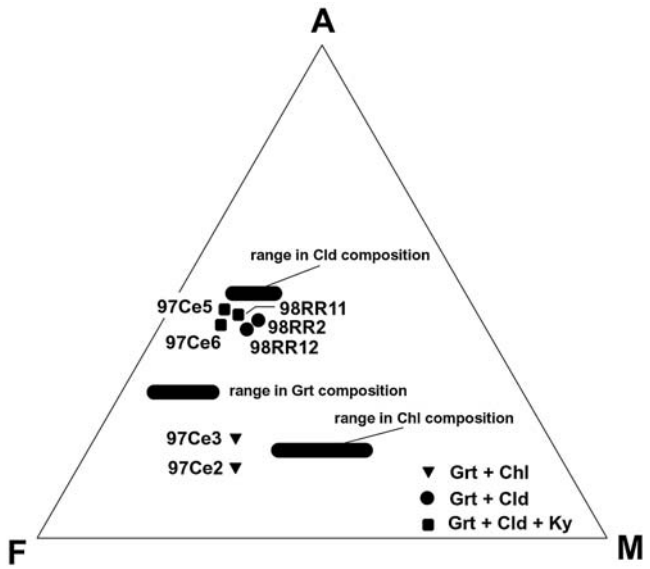

Fig. 4. AFM whole-rock chemistry projected from quartz, muscovite, paragonite and H_2O.

Garnet poikiloblasts contain inclusions of quartz, kyanite, chloritoid, graphite and rutile (Table 1). The poikiloblasts can show an internal schistosity (Si) mainly defined by minute graphite inclusions and small chloritoids (Fig. 3). The presence of sigmoidal structures in porphyroblasts and the continuity of internal (Si) and external (Se) schistosity (*i.e.* the main schistosity) (Zwart, 1960) indicate that garnet growth was pre-to-synkinematic with respect to the main schistosity (*i.e.* Se) (Fig. 2 and 3). Garnet microstructures are strikingly similar to those described by Stöckhert *et al.* (1997).

Three different generations of chloritoid are identified, namely (1) relict xenoblastic crystals included in the garnet; (2) xenoblastic to sub-idioblastic crystals dispersed in the matrix and aligned along the main schistosity; and (3) idioblastic chloritoid randomly oriented across the schistosity or pseudomorphing garnet. In most samples of kyanite-bearing schists, garnet is replaced by very fine-grained aggregates of randomly-oriented chloritoid associated with minute quartz grains. In kyanite-free samples, garnet is replaced by chlorite-chloritoid aggregates. Chlorite is present as idioblastic synkinematic crystals or as secondary minerals in pseudomorphic aggregates after garnet and/or chloritoid (Table 1, Fig. 2). Kyanite is observed as inclusions defining the internal schistosity (Si) in the garnet and in the matrix (Table 1, Fig. 2 and 3b). It often shows a reaction rim consisting of chlorite and white mica (phengite), and also a pseudomorphic replacement by chloritoid and white mica. Graphite is mainly found in the grains whose growth began before the development of the main schistosity (Table1 and Fig. 2). Therefore, graphite may have been exhausted during the prograde metamorphic history, before or close to the peak P-T conditions. Rutile is present in all studied samples. Titanite is only found in sample 98RR10 as inclusions in garnet cores and is substituted by rutile in garnet rims and in the matrix.

To sum up, all the metapelites from the Raspas Complex contain quartz + white mica + rutile. Three synkinematic parageneses are distinguished, namely Grt+Cld+Ky, Grt+Cld and Grt+Chl. Late-kinematic phases include replacement of garnet and kyanite by chloritoid-quartz aggregates in the kyanite-bearing samples, and garnet replacement by chloritoid-chlorite aggregates in the kyanite-free samples.

Whole-rock chemistry

Whole-rock chemical analyses (Table 2) show that the metapelites have aluminium-rich and iron-rich compositions. In an AFM projection (Fig. 4), the analysed samples define three groups according to their parageneses.

Table 2. Whole-rock chemistry of metapelites from the Raspas Complex.

Assemblage	Grt+Cld+Ky			Grt+Cld		Grt+Chl	
Sample	98RR11	97Ce5	97Ce6	98RR2	98RR12	97Ce2	97Ce3
SiO_2	77.80	76.03	76.86	81.86	67.93	72.14	74.30
TiO_2	0.75	0.82	0.88	0.64	1.02	0.46	0.52
Al_2O_3	12.24	13.05	12.45	9.99	17.65	12.90	11.87
Fe_2O_3*	3.68	4.15	4.68	2.70	4.38	5.26	5.71
FeOcal	3.31	3.74	4.21	2.43	3.95	4.73	5.14
MnO	0.03	tr.	0.03	0.02	0.04	0.14	0.07
MgO	0.57	0.45	0.54	0.52	0.86	1.26	1.28
CaO	0.13	0.18	0.28	0.13	0.20	0.51	0.69
Na_2O	0.60	0.68	0.58	0.61	1.18	0.84	0.63
K_2O	1.33	1.31	1.27	1.06	1.91	2.22	1.88
P_2O_5	0.07	0.08	0.10	0.08	0.11	0.18	0.09
LOI	2.59	3.11	-	2.14	4.04	-	2.84
total**	99.80	99.86	97.67	99.75	99.32	95.91	99.88

*: all iron as Fe^{3+}; cal: calculated ($FeO=Fe_2O_3/1.111$); **: calculated using all iron as Fe^{3+}.

Grt+Chl samples are aluminium-poor compared to Grt+Cld+Ky and Grt+Cld samples. The latter are distinguished by their magnesium content, the Grt+Cld samples being more magnesium-rich than the Grt+Cld+Ky ones. The main variations in composition are due to the aluminium content, whereas a minor impact is related to the iron-magnesium ratio. This variation in the bulk rock chemistry suggests that the three different parageneses characterising the Raspas Complex metapelites are due to differences in the protolith composition rather than metamorphic conditions. Rare-earth element patterns of the garnet-chloritoid metapelites are similar to those of average pelites, indicating a continental source for the detrital material (Arculus *et al.*, 1999; Bosch *et al*., 2002).

Mineral chemistry

The chemical composition of white mica, garnet, chloritoid and chlorite were determined at the University of Lausanne, Switzerland, using the wavelength dispersive electron microprobe (CAMECA SX50). Complementary analyses have been performed with the Microsonde Ouest (Brest, France). In both cases, operating conditions were: 15 kV accelerating voltage and 15 nA sample current, after a calibration on natural mineral standards. Both simple point determinations and/or zoning profiles were obtained.

Garnet is characterised by a high almandine end-member content, averaging around 65 mol% (Table 3, Fig. 5). The zoning profile (Fig. 5b) shows a decreasing

Table 3. Representative electron microprobe analyses and structural formulae of garnet. Estimation of the Fe^{3+} content in garnet has been done on the basis of 24 oxygens and 16 cations (*e.g.* Spear, 1993). End-members have been calculated according to Deer *et al.* (1992).

Sample	97Ce5 (Grt+Cld+Ky)			98RR10 (Grt+Chl)		97Ce3 (Grt+Chl)	
	core	core	rim	core	rim	core	rim
Analysis	14	8	23	251	225	16	2
SiO_2	37.14	37.41	37.05	37.29	37.79	36.74	37.74
TiO_2	0.01	0.00	0.00	0.21	0.16	0.12	0.08
Al_2O_3	21.03	21.46	21.16	20.37	21.05	20.74	21.30
FeO*	35.44	34.37	34.31	29.38	30.08	32.65	29.75
MnO	0.42	0.44	0.35	2.73	0.14	0.62	0.49
MgO	1.98	3.53	3.31	0.61	3.00	2.52	5.43
CaO	4.86	3.76	3.79	9.96	8.45	6.77	5.75
Total	100.88	100.97	99.97	100.55	100.67	100.15	100.55
Numbers of ions on the basis of 16 cations and 24 oxygens							
Si	5.94	5.92	5.93	5.97	5.95	5.87	5.89
Al^{VI}	3.96	4.00	3.99	3.84	3.91	3.91	3.93
Fe^{3+}	0.16	0.16	0.15	0.16	0.14	0.32	0.27
Ti	0.00	0.00	0.00	0.03	0.02	0.02	0.01
Mg	0.47	0.83	0.79	0.15	0.70	0.60	1.26
Fe^{2+}	4.58	4.39	4.44	3.77	3.82	4.04	3.61
Mn	0.06	0.06	0.05	0.37	0.02	0.08	0.07
Ca	0.83	0.64	0.65	1.71	1.43	1.16	0.96
Total	16.00	16.00	16.00	16.00	16.00	16.00	16.00
Mol per cent end-members							
Almandine	77.1	74.2	74.9	62.9	64.0	68.7	61.2
Spessartine	1.0	1.0	0.8	6.2	0.3	1.4	1.1
Pyrope	7.9	14.1	13.3	2.4	11.8	10.2	21.4
Grossular	10.1	6.9	7.3	24.4	20.4	11.9	9.6
Andradite	4.0	3.9	3.7	4.1	3.5	7.8	6.7
X_{Mg}	0.09	0.16	0.15	0.04	0.16	0.13	0.26

*: all iron as Fe^{2+}; $X_{Mg}=Mg/(Mg+Fe^{2+})$

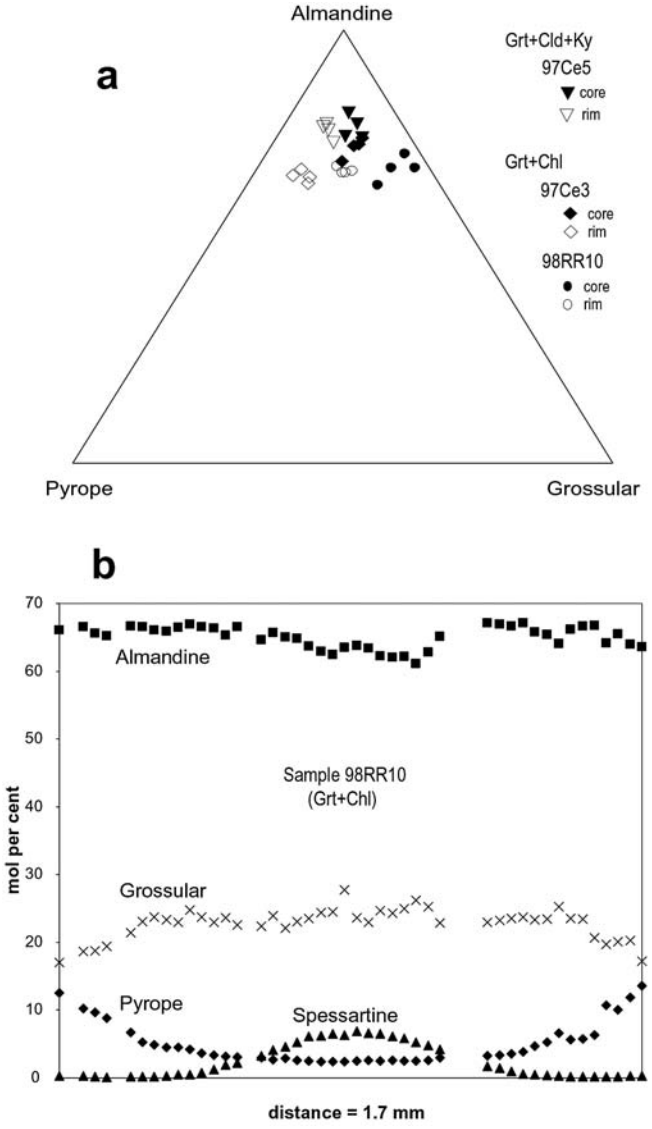

Fig. 5. (a) Garnet composition in terms of almandine, pyrope and grossular end-members. (b) Garnet zoning in sample RR 10 shows a smooth profile, with decreasing spessartine and grossular and increasing pyrope from core to rim. This profile is typical of growth zoning.

spessartine content and an increasing pyrope content from core to rim. The spessartine content decreases down to values less than 1 mol per cent in the outer part of the garnet porphyroblasts. Average variations in core and rim compositions are Alm60-76, Sps1-6, Prp2-9, Grs13-27 and Alm60-73, Sps0.3-1 Prp8-20, Grs15-23, respectively. All samples show a decreasing grossular content from core to rim, but garnet from sample 98RR10 shows a larger variation in grossular content compared to the other samples (Fig. 5a). This behaviour is consistent with the occurrence of titanite inclusions (instead of rutile) in garnet cores from sample 98RR10. The Mg/(Fe+Mg) ratio is higher in the samples 98RR10 and 97Ce3 compared to the sample 97Ce5, *i.e.* in the Grt+Chl paragenesis compared to the Grt+Cld+Ky paragenesis.

Chloritoid compositions change depending upon their microstructural site of growth (Table 4). Chloritoid inclusions (*i.e.* Cld-I) in garnet cores show a lower X_{Mg} with respect to chloritoid inclusions close to garnet rims (X_{Mg} varies from 0.11 to 0.18). Matrix chloritoid (*i.e.* Cld-II) is slightly more magnesian (X_{Mg} = 0.21-0.23) than the most magnesian inclusions in the garnet grains, while the randomly-oriented grains (*i.e.* Cld-IIIb) in the matrix and the chloritoid grains pseudomorphing garnet (*i.e.* Cld-IIIa) are less magnesian (X_{Mg} = 0.15-0.21). Synkinematic chlorites (*i.e.* Chl-II) are richer in Si and Mg (X_{Mg} = 0.43-0.58) than post-kinematic chlorites (*i.e.* Chl-III) (X_{Mg} = 0.33-0.36) growing at the expense of garnet or chloritoid (Table 5).

White mica is phengitic muscovite, except in sample 97Ce3 where paragonite has also been found. Phengite displays a relatively high Si content (from 6.30 to 6.72 atoms p.f.u on the basis of 22 oxygen) and the Mg+Fe(tot) content varies between 0.35 and 1.08 atoms p.f.u. (Table 6 and Fig. 6). All the studied samples, except 98RR10, are graphite-bearing metapelites, suggesting that relatively low fO_2 conditions prevailed during most of the prograde history. Accordingly we assume that all iron is divalent (Guidotti, 1984). In addition, analyses of phengite from graphite-bearing samples plot close to the ideal Tschermak substitution, suggesting that a negligible amount of ferric iron is present (Guidotti, 1984; Spear, 1993). If graphite is lacking (sample 98RR10), the analyses plot significantly above the ideal substitution (Fig. 6), indicating that a significant amount of ferric iron is present. The Si content is higher in chloritoid-free samples (Si = 6.45-6.60 pfu) than in chloritoid-bearing samples (Si = 6.35-6.45 pfu). Phengite grains are locally slightly zoned, with decreasing Si-content from core to rim.

Reaction history of the Raspas metapelites

Mineral assemblages and compositions from the Raspas micaschists are shown in an Al_2O_3-FeO-MgO (AFM) projection assuming excess quartz, muscovite and water (Thompson, 1957) (Fig. 7 and 8). Phase relations between observed phases are best illustrated in the SiO_2-Al_2O_3-FeO-MgO-K_2O-H_2O (KFMASH) system (Fig. 9). Few topologies are possible in this multisystem, due to numerous experimental data in the limiting FASH system (Rao & Johannes, 1979). Theoretical and calculated grids show two alternatives, whether staurolite is more magnesian than coexisting garnet (Harte & Hudson, 1979; Spear, 1999) or *vice-versa* (Chopin, 1984; Ballèvre *et al*., 1989; Powell & Holland, 1990). Empirical (*e.g.* Harte & Hudson, 1979; Vuichard & Ballèvre, 1988; Ballèvre *et al*., 1989) as well as calculated KFMASH (*e.g.* Powell & Holland, 1990; Powell *et al*., 1998; Spear, 1999) grids show that the assemblage garnet-chloritoid-kyanite is stable within a narrow temperature range at high pressure.

Possible P-T paths in the KFMASH system

Possible P-T paths for the Raspas metapelites will be discussed first in the model KFMASH system (Fig. 9).

Table 4. Representative electron microprobe analyses and structural formulae of chloritoid. Estimation of the Fe^{3+} content in chloritoid has been done assuming stoichiometry, *i.e.* $Fe^{3+} = 4-(Ti^{4+}+Al^{3+})$ (Deer *et al*., 1992).

Sample	98RR11 (Grt+Cld+Ky)		97Ce5 (Grt+Cld+Ky)				98RR2 (Grt+Cld)			98RR12 (Grt+Cld)		
Generation	II	IIIb	I	I	II	IIIb	II	IIIa	IIIb	II	IIIa	IIIb
Analysis	36	35	11	7	32	57	11	23	10	45	15	40
SiO_2	24.44	24.23	24.23	24.48	25.00	24.30	24.09	24.10	24.39	23.91	24.13	23.91
TiO_2	0.00	0.00	0.00	0.00	0.00	0.00	0.00	0.00	0.00	0.00	0.10	0.00
Al_2O_3	41.27	41.06	40.07	40.69	41.04	40.24	41.01	40.70	41.11	40.78	41.04	40.76
FeO*	23.54	24.30	26.31	24.40	22.83	24.63	23.17	25.16	23.08	24.33	24.63	24.23
MnO	0.08	0.25	0.12	0.06	0.03	0.21	0.18	0.23	0.34	0.22	0.34	0.34
MgO	3.45	3.07	1.76	2.98	3.66	2.55	3.87	2.49	3.39	3.05	2.57	2.85
Total	92.79	92.93	92.54	92.62	92.58	91.94	92.33	92.72	92.37	92.33	92.84	92.13
Numbers of ions on the basis of 12 O												
Si	2.00	1.99	2.01	2.01	2.03	2.02	1.98	1.99	2.00	1.98	1.99	1.98
Al	3.00	3.00	3.00	3.00	3.00	3.00	3.00	3.00	3.00	3.00	3.00	3.00
Al	0.98	0.97	0.93	0.95	0.95	0.94	0.97	0.97	0.98	0.98	0.98	0.98
Ti	0.00	0.00	0.00	0.00	0.00	0.00	0.00	0.00	0.00	0.00	0.00	0.00
Fe^{3+}	0.02	0.03	0.07	0.05	0.05	0.06	0.03	0.03	0.02	0.02	0.02	0.02
Fe^{2+}	1.58	1.64	1.76	1.62	1.50	1.65	1.56	1.71	1.56	1.66	1.69	1.67
Mn	0.00	0.01	0.00	0.00	0.00	0.00	0.01	0.02	0.02	0.01	0.02	0.02
Mg	0.42	0.37	0.22	0.36	0.44	0.31	0.47	0.31	0.42	0.37	0.31	0.35
Total	8.00	8.01	7.99	7.99	7.98	7.98	8.03	8.02	8.01	8.02	8.01	8.02
X_{Fe}	0.79	0.81	0.89	0.82	0.77	0.83	0.76	0.84	0.78	0.81	0.83	0.82
X_{Mn}	0.00	0.01	0.00	0.00	0.00	0.01	0.01	0.01	0.01	0.01	0.01	0.01
X_{Mg}	0.21	0.18	0.11	0.18	0.23	0.16	0.23	0.15	0.21	0.18	0.16	0.17

*: all iron as Fe^{2+}; $X_{Fe}=Fe^{2+}/(Mg+Mn+Fe^{2+})$; $X_{Mn}=Mn/(Mg+Mn+Fe^{2+})$; $X_{Mg}=Mg/(Mg+Mn+Fe^{2+})$

According to the KFMASH grids calculated by Powell & Holland (1990) and Powell *et al*. (1998), the assemblage Grt-Cld-Ky is stable at higher pressures than the KFMASH invariant point (*i.e.* at about 12 kbar), in a narrow temperature interval (560-600°C). Specifically, the lower temperature limit of the Grt-Cld-Ky assemblage is defined by the incoming of almandine + kyanite at the expense of Fe-chloritoid + quartz, and the upper temperature limit by the breakdown of chloritoid through the KFMASH univariant reaction Cld = Grt + Chl + Ky +V.

The P-T evolution of the Raspas metapelites can be described in this simplified model by path A (continuous line on fig. 9). Garnet and chloritoid coexisting with kyanite in sample 97Ce5 (Figs. 7 and 8) show increasing

Table 5. Representative electron microprobe analyses and structural formulae of chlorite. All iron is assumed to be divalent.

Sample	98RR2 (Grt+Cld)		98RR12 (Grt+Cld)			98RR10 (Grt+Chl)			97Ce3 (Grt+Chl)		
	core	rim	core	rim	max. Mg	core	rim	min. Mg	core	rim	min. Mg
Analysis	27	26	16	17	12	30	27	33	59	54	64
SiO_2	23.43	23.74	23.44	23.31	24.07	26.70	26.48	29.40	26.20	25.76	26.27
TiO_2	0.07	0.05	0.08	0.11	0.05	0.07	0.07	0.11	0.05	0.03	0.07
Al_2O_3	21.62	21.41	21.07	21.63	20.90	20.01	19.93	19.38	21.49	21.23	21.17
Cr_2O_3	0.01	0.05	0.01	0.05	0.01	0.03	0.01	0.03	0.05	0.04	0.03
FeO*	31.97	32.62	33.21	33.67	32.62	23.68	24.18	23.64	23.09	24.71	28.65
MnO	0.17	0.13	0.17	0.15	0.16	0.00	0.02	0.04	0.05	0.03	0.17
MgO	10.16	10.39	9.05	9.41	9.99	18.08	16.91	14.49	17.40	15.95	11.94
CaO	0.00	0.03	0.00	0.07	0.04	0.02	0.03	0.15	0.01	0.00	0.10
Na_2O	0.00	0.01	0.03	0.02	0.00	0.03	0.02	0.03	0.02	0.01	0.01
K_2O	0.00	0.02	0.01	0.00	0.01	0.02	0.02	0.35	0.03	0.01	0.01
Total	87.42	88.45	87.08	88.42	87.84	88.64	87.67	87.61	88.38	87.77	88.43
Numbers of ions on the basis of 28 O											
Si	5.16	5.18	5.22	5.12	5.28	5.51	5.54	6.09	5.40	5.40	5.57
Al^{IV}	2.84	2.82	2.78	2.88	2.72	2.49	2.46	1.91	2.60	2.60	2.43
Al^{VI}	2.77	2.68	2.75	2.72	2.69	2.37	2.46	2.83	2.62	2.64	2.85
Ti	0.01	0.01	0.01	0.02	0.01	0.01	0.01	0.02	0.01	0.01	0.01
Cr	0.00	0.01	0.00	0.01	0.00	0.01	0.00	0.00	0.01	0.01	0.00
Fe*	5.89	5.95	6.19	6.18	5.99	4.08	4.23	4.10	3.98	4.33	5.08
Mn	0.03	0.02	0.03	0.03	0.03	0.00	0.00	0.01	0.01	0.01	0.03
Mg	3.33	3.38	3.00	3.08	3.27	5.56	5.27	4.48	5.34	4.98	3.77
Ca	0.00	0.01	0.00	0.02	0.01	0.01	0.01	0.03	0.00	0.00	0.02
Na	0.00	0.00	0.01	0.01	0.00	0.01	0.01	0.01	0.01	0.00	0.00
K	0.00	0.01	0.00	0.00	0.00	0.01	0.00	0.09	0.01	0.00	0.00
Total	20.03	20.06	20.01	20.06	20.00	20.05	20.00	19.57	19.99	19.98	19.78
X_{Mg}	0.36	0.36	0.33	0.33	0.35	0.58	0.55	0.52	0.57	0.53	0.43

*: all iron as Fe^{2+}; $X_{Mg}=Mg/(Mg+Fe^{*})$

Table 6. Representative electron microprobe analyses and structural formulae of white micas. All iron is assumed to be divalent.

	Grt+Cld+Ky		Grt+Cld			Grt+Chl		
Sample	98RR11	97Ce5	98RR2	98RR12		98RR10	97Ce3	
	phengite	phengite	phengite	phengite	paragonite	phengite	phengite	paragonite
Analysis	27	43	6	30	5	44	5	8
SiO_2	48.21	48.52	48.00	47.60	46.63	48.58	49.08	46.34
TiO_2	0.47	0.44	0.45	0.48	0.11	0.94	0.43	0.11
Al_2O_3	33.12	32.45	33.16	33.16	38.79	26.51	30.97	39.45
Cr_2O_3	0.00	0.06	0.04	0.02	0.08	0.14	0.03	0.05
FeO*	1.44	1.34	1.35	1.27	0.49	2.65	1.30	0.26
MnO	0.00	0.01	0.03	0.03	0.01	0.04	0.02	0.00
MgO	1.61	1.62	1.69	1.65	0.13	3.72	2.51	0.17
CaO	0.02	0.00	0.02	0.00	0.31	0.00	0.00	0.33
Na_2O	1.10	1.21	1.37	1.31	6.79	0.53	1.06	7.08
K_2O	8.54	8.94	8.73	8.68	1.26	9.99	8.83	0.95
Total	94.52	94.60	94.84	94.20	94.60	93.10	94.22	94.74
Numbers of ions on the basis of 22 O								
Si	6.40	6.45	6.36	6.35	6.02	6.67	6.54	5.96
Al^{IV}	1.60	1.55	1.64	1.65	1.98	1.33	1.46	2.04
Al^{VI}	3.57	3.53	3.55	3.56	3.92	2.96	3.41	3.95
Ti	0.05	0.04	0.05	0.05	0.01	0.10	0.04	0.01
Cr	0.00	0.01	0.00	0.00	0.01	0.02	0.00	0.01
Fe*	0.16	0.15	0.15	0.14	0.05	0.30	0.15	0.03
Mn	0.00	0.00	0.00	0.00	0.00	0.01	0.00	0.00
Mg	0.32	0.32	0.33	0.33	0.03	0.76	0.50	0.03
Ca	0.00	0.00	0.00	0.00	0.04	0.00	0.00	0.05
Na	0.28	0.31	0.35	0.34	1.70	0.14	0.27	1.77
K	1.44	1.52	1.48	1.48	0.21	1.75	1.50	0.16
Total	13.83	13.88	13.91	13.90	13.97	14.03	13.87	13.99

*: all iron as Fe^{2+}

X_{Mg}, indicating increasing temperature during garnet growth. This records part of the prograde P-T path, ideally taking place over a short temperature interval, of the order of 20°C. The other peak parageneses observed (Table 1 and Fig. 7 and 8), namely garnet + chloritoid and garnet + chlorite are trivariant in the KFMASH system. Peak P-T conditions are located within the shaded area in Fig. 9.

Retrograde phases include chloritoid + quartz in kyanite-bearing rocks and chloritoid + chlorite in kyanite-absent samples. These two retrograde assemblages document back-reaction along the two divariant reactions, Grt+Ky = Cld+Qtz and Grt = Cld+Chl, respectively (Fig. 9). In both reactions, the amount of retrograde products will depend upon the amount of available H_2O. Two cases are to be considered. First, if $a(H_2O) = 1$ throughout decompression, the P-T path during decompression should cross the bounding FASH reaction above the KFASH invariant point, *i.e.* above 15 kbar. This places severe constraints on the shape of the P-T path, indicating decreasing temperatures during the earliest stage of the decompression. Second, the

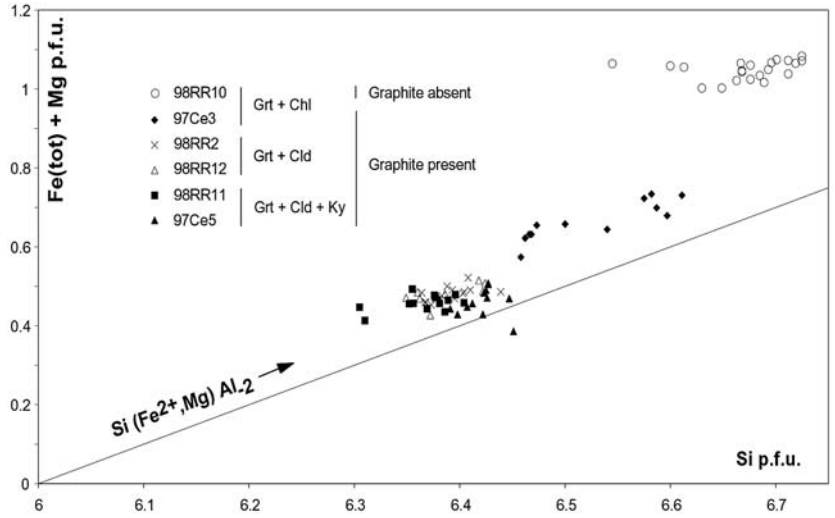

Fig. 6. Phengite chemistry in terms of Si content (on the basis of 22 oxygens) and Fe(total)+Mg content. The line represents the ideal inverse Tschermak substitution.

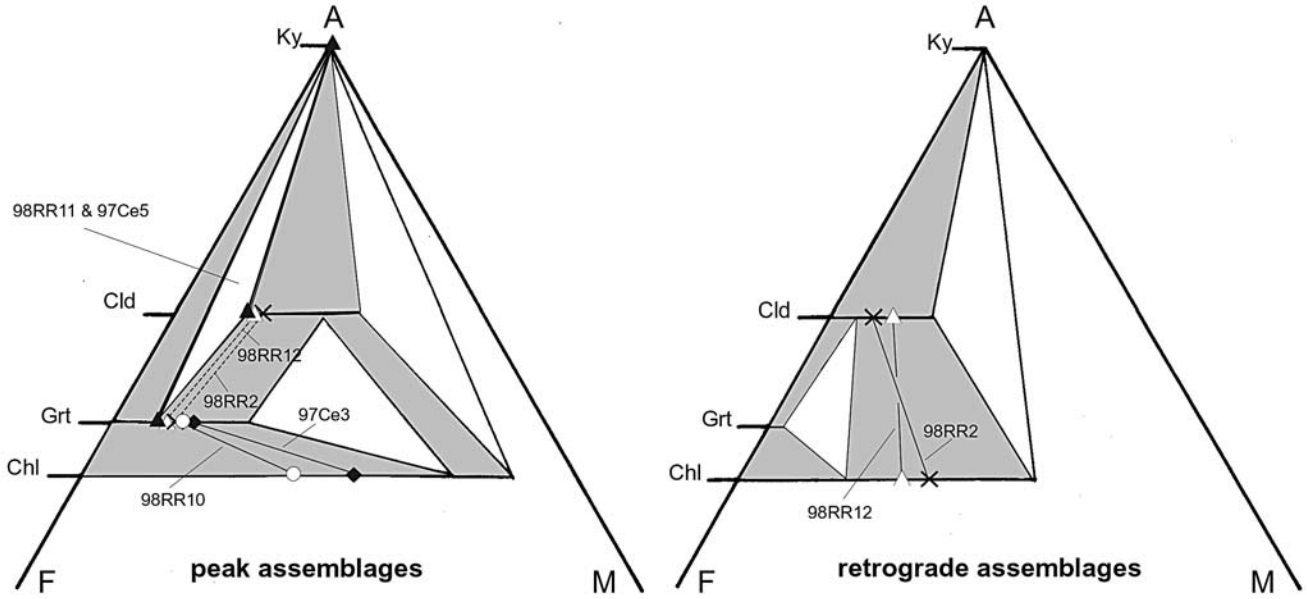

Fig. 7. AFM projection of coexisting minerals in the Raspas metapelites. Peak assemblages are depicted using measured compositions (full lines), and assumed compositions when garnet is totally pseudomorphed (dashed lines). Crossing tie-lines for retrograde assemblages indicate disequilibrium or growth at different P-T conditions in the two investigated samples. The grey fields indicate the extent of trivariant assemblages in the AFM diagram.

assumption of a unit activity for H_2O during decompression is unlikely. Decreasing the a(H_2O) displaces the divariant equilibria towards lower temperatures. Consequently, the garnet breakdown reaction could have taken place at a lower pressure than the KFASH invariant point, but still at higher pressures than the location of the Alm-St-Cld-Ky invariant point for the corresponding a(H_2O) (open circle in Fig. 9). This would also indicate decreasing temperature at an early stage of the decompression.

Possible P-T paths in the KFMnMASH system

The model KFMASH system needs some refinement, for two main reasons. First, because of the presence of graphite, the activity of H_2O in the fluid phase is expected to be slightly lower than 1, resulting in all fluid-bearing equilibria being displaced towards lower temperatures. Second, the incorporation of MnO into garnet displaces the KFASH invariant point towards lower P-T, ideally along the Grt-absent reaction if MnO only enters garnet or if X_{Mn} (Cld) = X_{Mn} (St), neither of these limiting assumptions being strictly true (Droop & Harte, 1995). Moreover, MnO will stabilise the KFMnMASH reaction Cld+Ky = Grt+St+Chl+V (Fig. 9), and the corresponding KFMASH reactions will become divariant. Accordingly, the equilibrium curves bounding the garnet-chloritoid-kyanite stability field will be displaced towards lower temperatures, potentially greatly extending the stability field of the assemblage Grt-Cld-Ky (Fig. 9).

The main consequence for the possible P-T paths of the Raspas metapelites is that peak temperatures could potentially be at lower temperature than the KFASH equilibria Cld+Qtz = Alm+Ky+V (dashed line on Fig. 9). The change in chemistry during garnet growth is interpreted in the same manner than discussed above in the pure KFMASH system, indicating increasing temperature during garnet growth but at lower absolute values. As also discussed above, the retrograde reactions could indicate two types of

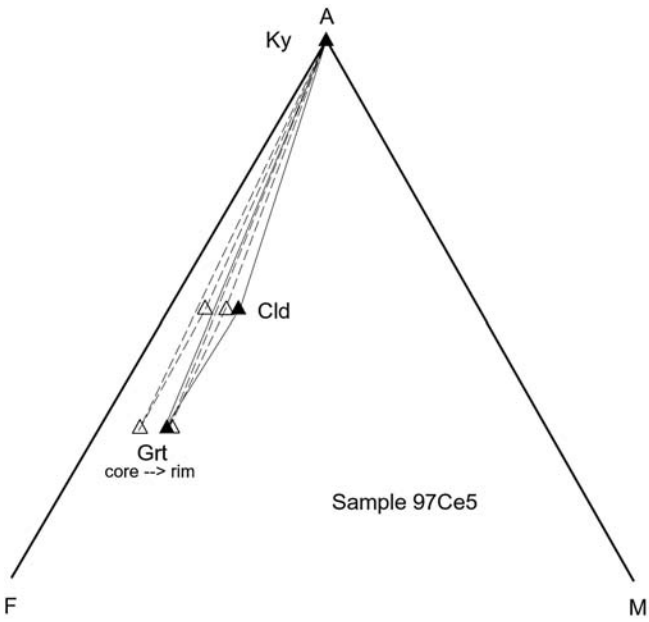

Fig. 8. AFM projection showing the prograde evolution of the Grt-Cld-Ky assemblage. The displacement of the three-phase field towards higher magnesian compositions is recorded by chloritoid (and kyanite) inclusions within garnet (open symbols), then matrix chloritoid coexisting with garnet rims (filled symbols).

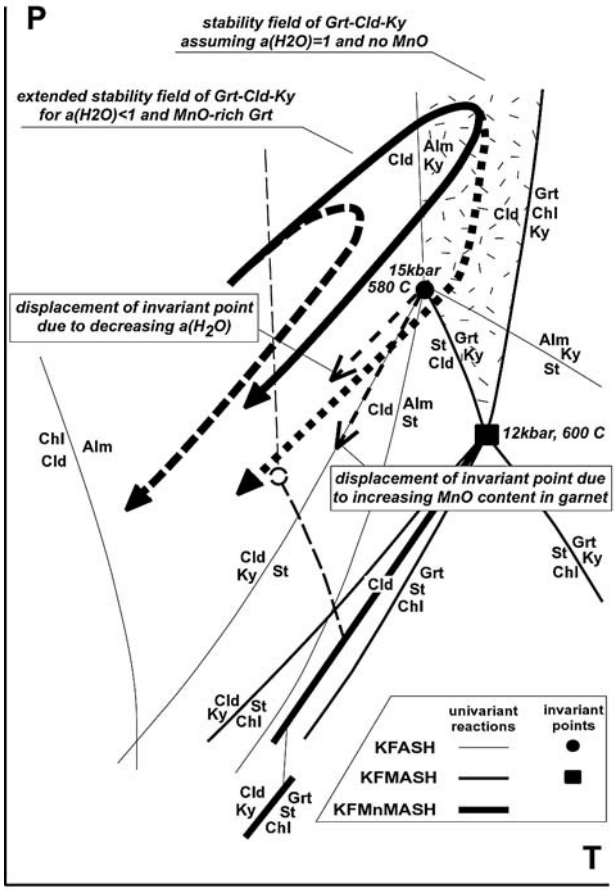

Fig. 9. Possible P-T path for the Raspas metapelites. The topology of the KFMASH grid is taken from Powell & Holland (1990). Note the narrow stability field of the Grt-Cld-Ky assemblage, provided that garnet does not contain a significant amount of spessartine and assuming a unit H_2O activity. The continuous line describes the simplest P-T path. Increasing the spessartine content in garnet and/or decreasing the H_2O activity displace the KFASH invariant point (filled circle) towards lower P-T. Accordingly, the stability field of the trivariant assemblage Grt-Cld-Ky is extended towards lower P-T conditions. Taking these additional complexities into account, two other P-T paths (short- and long-dashed lines) are possible (see text for further discussion). Note that conventional thermometry, indicating high temperatures of equilibration, would favour the simplest P-T path.

P-T paths, both requiring a temperature decrease at an early stage of the decompression.

Although potentially significant, the effect of MnO is considered minor in the Raspas metapelites because of the observed mineral compositions: the spessartine content in garnet rims does not exceed 1.1 mole per cent (Table 3 and Fig. 5b), and the X_{Mn} in chloritoid is equal or lower to 0.01 (Table 4).

Estimation of peak P-T conditions

Few geothermobarometers can be applied in the Raspas metapelites (Table 7). The $FeMg_{-1}$ exchange between garnet and phengite is an experimentally-calibrated thermometer (Green & Hellman, 1982). Application of this thermometer in rocks is limited by the problem of determination of the ferric iron in phengite. In the studied samples, this is not considered as a serious limitation, because the presence of graphite suggests low oxidation conditions. Results of calculations in three samples (Table 7) indicate temperatures for the peak metamorphism of the order of 620-650°C at a nominal pressure of 15 kbar. Because of the assumption that all the iron is divalent, the calculated temperatures represent maximum values. Assuming 10 % of the iron is ferric, the estimated temperatures decrease by 5-10°C, an amount smaller than the uncertainty associated to the calibration itself. The empirically-calibrated $Fe\text{-}Mg_{-1}$ exchange between garnet and chlorite (Dickenson & Hewitt, 1986, modified in Laird, 1988; Grambling, 1990; Perchuk, 1991) give temperatures of 580-620°C for samples 98RR10 and 97Ce3 (Table 7). On the whole, the garnet-phengite thermometer gives temperatures 0-50°C higher than the garnet-chlorite thermometer. The chloritoid-chlorite geothermometer (Vidal *et al*., 1999) can be used for the retrograde assemblages in the kyanite-absent samples. The temperatures calculated are much higher than expected, possibly because of disequilibrium.

Although pressure estimates are difficult, maximum values are indicated by the stability of paragonite, which is defined by the reaction Pg = Jd + Ky at approximately 25 kbar (Holland, 1979a). Experimental data on the assemblage Alm-Ky-Phe in the KFASH system (Massonne & Szpurka, 1997) indicates pressures of the order of 20 kbar (at 600°C). The uncertainty associated with this estimation is probably quite large, because a minor variation along the $SiMgAl_{-2}$ exchange is accompanied by a significant change in pressure.

A phase diagram approach has been used for garnet-chloritoid-kyanite parageneses by Konopasek (2001), who has calculated the topology of the KFMASH system using the Vertex software (Connolly, 1990). According to his calculations, peak P-T conditions in sample 97Ce5 would be at about 15 kbar, 580°C.

On the whole, conventional and multiequilibrium thermobarometry suggest P-T conditions of the order of 20 ± 5 kbar, 550 ± 50°C. The temperature value is far better constrained than the pressure value. The temperatures obtained using the H_2O-independent exchange reactions are not significantly lower than those predicted by the KFMASH grid, showing that the uncertainties associated with the minor components are negligible or, at best, smaller than the uncertainties associated to the calculation procedures used for P-T estimations. The P-T values reported in this study for the Raspas Complex are not very different from those calculated by Feininger (1980), *i.e.* 13 ± 3 kbar at 580 ± 20°C but are significantly higher than those proposed by Duque (1993), *i.e.* 9 ± 0.5 kbar and 460 ± 30°C. Duque (1993) used the equilibrium garnet-plagioclase-kyanite-quartz in the metapelites and plagioclase-omphacite-quartz in the metabasites for estimating peak pressures, assuming that plagioclase was in equilibrium with the other minerals. Because plagioclase is lacking in both the metapelites and the eclogites, and because plagio-

Table 7. Summary of geothermometric calculations at a nominal pressure of 15 kbar.

Conventional thermometry		98RR10 (°C)	97Ce3 (°C)	97Ce5 (°C)	98RR2 (°C)	98RR12 (°C)
Grt-Phe	Green & Hellman (1982)	617	646	617		
Grt-Chl	Laird (1988)	617	600			
	Grambling (1990)	585	573			
	Perchuk (1991)	584	576			
Cld-Chl	Vidal et al. (1999)				649*	668*

Abbreviations are after Kretz (1983); in addition Phe, phengite;
* Cld and Chl are post-kinematic (generation III).

clase is a late, retrograde phase, in the blueschists (Feininger, 1980), Duque's estimations should be considered as minimum pressures for the eclogite-facies event.

Discussion

Metapelitic rocks are sensitive recorders of P-T paths in high-pressure terranes. To a first approximation, the KFMASH grid as calculated by Powell & Holland (1990) is a primary tool for describing the P-T paths (Fig. 9). Although minor departures from the KFMASH grid can be expected due to incorporation of MnO and CaO into garnet and the effect of variable water and oxygen fugacities, three main types of assemblages are recorded, briefly described below in order of increasing peak temperature.

At relatively low temperatures, the Grt-Cld-Chl assemblage is stable. As recorded in numerous blueschist-facies terranes, for example in the Seward Peninsula, Alaska (Thurston, 1985; Patrick & Evans, 1989), New Caledonia (Ghent *et al*., 1987), the western Alps (Vuichard & Ballèvre, 1988) and the Variscan belt (Guiraud *et al*., 1987; Bosse *et al*., 2002). Garnet-chloritoid metapelites are generally associated with garnet-bearing blueschists and low-temperature, glaucophane-bearing, eclogites. Because the divariant reaction Cld = Grt + Ky has not been attained, kyanite is lacking in the garnet-chloritoid metapelites.

At slightly higher temperatures, the divariant reaction Cld = Grt + Ky allows kyanite to develop in the most iron-rich bulk-rock compositions. Four occurrences of Grt-Cld-Ky micaschists are known to the authors, namely the Raspas Complex (Feininger, 1980; this study), the Sesia zone, western Alps (Pognante *et al.*, 1980; Vuichard & Ballèvre, 1988; Zucali *et al*., 2002), the Tauern window, eastern Alps (Holland, 1979b; Miller, 1986; Spear & Franz, 1986; Stöckhert *et al*., 1997) and the Bohemian Massif (Konopasek, 2001). In these four occurrences, garnet-chloritoid-kyanite micaschists are associated with garnet-omphacite-amphibole eclogites, the amphibole being a glaucophane and/or a barroisite, or a barroisite rimmed by glaucophane (Raspas Complex: Gabriele, 2002; Sesia Zone: Koons, 1982; Tropper & Essene, 2002). The P-T estimates in these areas are at about 17-21 kbar, 550-650 °C in the Sesia Zone (*e.g.* Tropper *et al*., 1999; Tropper & Essene, 2002), 20 kbar, 600 ± 20°C in the Tauern Window (Holland, 1979b). In this latter locality, chloritoid growth at the expense of garnet has been described (Holland, 1979b). Chloritoid-quartz aggregates replacing garnet and kyanite have been reported in the Sesia Zone, western Alps (Vuichard & Ballèvre, 1989), and the Raspas Complex (see above). These textures basically indicate decreasing temperatures during decompression, and are consistent with glaucophane overgrowths on barroisite (Koons, 1982; Tropper & Essene, 2002; Gabriele, 2002).

At still higher temperatures, Grt-Cld-Ky was a stable assemblage during part of the prograde, up-temperature, history, but the chloritoid stability was exceeded resulting in Grt-Ky, Grt-Chl-Ky or Grt-Tlc-Ky assemblages. Chloritoid is thus found only as inclusions in garnet cores. Examples include the ultra-high pressure Dora-Maira massif in the western Alps (Chopin, 1984; Compagnoni *et al*., 1995; Simon *et al*., 1997; Compagnoni & Hirajima, 2001), the high-pressure Champtoceaux Complex in the Variscan belt (Ballèvre *et al*., 1989; Ballèvre & Marchand, 1991; Bosse *et al.*, 2000) and the Adula Nappe in the central Alps (Meyre *et al*., 1999). Associated eclogites are characterized by barroisitic amphiboles, glaucophane being restricted to highly sodic and magnesian bulk-rock compositions (Kiénast *et al*., 1991).

Acknowledgments: The logistic support of the Institut de Recherche et Développement was of invaluable help during field work in Ecuador. The Swiss National Science Foundation supported this study through grant 20-50812.97. J. Aspden is thanked for indicating possible sample localities in the Raspas Complex at an early stage of this work. The authors are also greatly indebted to H. Lapierre for providing whole-rock chemical analyses of some samples of metapelites from the Raspas Complex. Critical reviews of this manuscript by G.T.R. Droop, D. Lattard and an anonymous petrologist are gratefully acknowledged.

References

Arculus, R.J., Lapierre, H., Jaillard, E. (1999): Geochemical window into subduction and accretion processes: Raspas metamorphic complex, Ecuador. *Geology*, **27**, 547-550.

Aspden, J.A. & McCourt, W.J. (1986): Mesozoic oceanic terrane in the central Andes of Colombia. *Geology*, **14**, 415-418.

Aspden, J.A., McCourt, W.J., Brook, M. (1987): Geometrical control of subduction-related magmatism: the Mesozoic and

Cenozoic plutonic history of Western Colombia. *J. Geol. Soc. London*, **144**, 893-905.

Aspden, J. A., Bonilla, W., Duque, P. (1995): The El Oro metamorphic complex, Ecuador: geology and economic mineral deposits. British Geological Survey, Keyworth, UK. *Overseas Geology and Mineral Resources*, **67**, 1-63.

Ballèvre, M. & Marchand, J. (1991): Zonation du métamorphisme éclogitique dans la nappe de Champtoceaux (Massif armoricain, France). *C. R. Acad. Sci. Paris*, **(II) 312**, 705-711.

Ballèvre, M., Pinardon, J.-L., Kiénast, J.-R., Vuichard, J.-P. (1989): Reversal of Fe-Mg partinioning between garnet and staurolite in eclogite-facies metapelites from the Champtoceaux Nappe (Britanny, France*). J. Petrol.*, **30**, 1321-1349.

Bosch, D., Gabriele, P., Lapierre, H., Malfère, J.-L., Jaillard, E. (2002): Geodynamic significance of the Raspas Metamorphic Complex (SW Ecuador): geochemical and isotopic constraints. *Tectonophysics*, **345**, 83-102.

Bosse, V., Féraud, G., Ruffet, G., Ballèvre, M., Peucat, J.-J., de Jong, K. (2000): Late Devonian subduction and early-orogenic exhumation of eclogite-facies rocks from the Champtoceaux Complex (Variscan belt, France). *Geol. J.*, **35**, 297-325.

Bosse, V., Ballèvre, M., Vidal, O. (2002): Ductile thrusting recorded by the garnet isograd in the blueschist-facies metapelites from the Ile de Groix (Armorican Massif, France). *J. Petrol.*, **43**, 485-510.

Chopin, C. (1984): Coesite and pure pyrope in high-grade blueschists of the Western Alps; a first record and some consequences. *Contrib. Mineral. Petrol.*, **86**, 107-118.

Compagnoni, R. & Hirajima T. (2001): Superzoned garnets in the coesite-bearing Brossasco-Isasca Unit, Dora-Maira massif, Western Alps, and the origin of the whiteschists. *Lithos*, **57**, 219-236.

Compagnoni, R., Dal Piaz, G.V., Hunziker, J.C., Gosso, G., Lombardo, B., Williams, P. (1977): The Sesia-Lanzo zone, a slice of continental crust with alpine high pressure-low temperature assemblages in the Western Italian Alps. *Rend. Soc. Ital. Min. Petr*., **33**, 281-334.

Compagnoni, R., Hirajima, T., Chopin, C. (1995): Ultra-high pressure metamorphic rocks in the western Alps. *in* "Ultrahigh pressure metamorphism", Coleman, R.G. & Wang, X eds., Cambridge University Press, 206-243.

Connolly, J.A.D. (1990): Multivariable phase diagrams: an algorithm based on genralized thermodynamics. *Am. J. Sci.*, **290**, 666-718.

Deer, W.A., Howie, R.A., Zussman, J. (1992): An Introduction to the Rock-Forming Minerals, 2nd edition. Longman Scientific & Technical, London, 696 p.

De Souza, H.-A.-F, Espinosa, A., Delaloye, M. (1984): K-Ar ages of basic rocks in the Patia Valley, Southwest Colombia. *Tectonophysics*, **107**, 135-145.

Dickenson, M.P. & Hewitt, D.A. (1986): A garnet-chlorite geothermometer. *Geol. Soc. America*, *Abs. and Prog.*, **18**, 584.

Droop, G.T.R. & Harte, B. (1995). The effect of Mn on the phase relations of medium-grade pelites: constraints from natural assemblages on petrogenetic grid topology. *J. Petrol*., **36**, 1549-1578.

Duque, P. (1993): Petrology, metamorphic history and structure of El Oro Ophiolitic Complex, Ecuador. Second ISAG, *International Symposium on Andean Geodynamics*, Oxford (UK), Extended Abstracts Volume, 359-362.

Ernst, W.G. (1973): Blueschist metamorphism and P-T regimes in active subduction zones. *Tectonophysics*, **17**, 255-272.

Feininger, T. (1978): Geologic map of western El Oro Province. 1/50000. Escuela Politecnica Nacional, Quito, Ecuador.

— (1980): Eclogite and related high-pressure regional metamorphic rocks from the Andes of Ecuador. *J. Petrol.*, **21**, 107-140.

— (1982a): Glaucophane schists in the Andes at Jambalo, Colombia. *Can. Mineral.*, **20**, 41-47.

— (1982b): The metamorphic "basement" of Ecuador. *Geol. Soc. Am. Bull.*, **93**, 87-92.

— (1987): Allochtonous terranes in the Andes of Ecuador and northwestern Peru. *Can. J. Earth Sci.*, **24**, 266-278.

Feininger, T. & Bristow, C.R. (1980): Cretaceous and Paleogene geologic history of coastal Ecuador. *Geol. Rundsch.*, **69**, 849-874.

Gabriele, P. (2002): HP terranes exhumation in an active margin setting: geology, petrology and geochemistry of the Raspas Complex in SW Ecuador. Unpublished Ph.D. Thesis, University of Lausanne, Switzerland.

Gansser, A. (1973): Facts and theories on the Andes. *J. Geol. Soc. London*, **129**, 93-131.

Ghent, E.D., Stout, M.V., Black, P., Brothers, R.N. (1987). Chloritoid-bearing rocks associated with blueschists and eclogites, northern New Caledonia. *J. metamorphic Geol.*, **5**, 239-254.

Grambling, J.A. (1990): Internally-consistent geothermobarometry and H_2O barometry in metamorphic rocks: the example garnet-chlorite-quartz. *Contrib. Mineral. Petrol.*, **105**, 617-628.

Green, T.H. & Hellman, P.L. (1982): Fe-Mg partitioning between coexisting garnet and phengite at high pressure, and comments on a garnet-phengite geothermometer. *Lithos*, **15**, 253-266.

Guidotti, C.V. (1984): Micas in metamorphic rocks. *Reviews in Mineralogy*, **13**, 357-467.

Guiraud, M., Burg, J.-P., Powell, R. (1987): Evidence for a Variscan suture zone in the Vendée, France: a petrological study of blueschist facies rocks from Bois de Cené. *J. metamorphic Geol.*, **5**, 225-237.

Harte, B. & Hudson, N.F.C. (1979): Pelite facies series and pressures of Dalradian metamorphism in E-Scotland. *in* "The Caledonides of the British Isles; Reviewed", A.L. Harris, C.H. Holland, B.E. Leake eds., *Geol. Soc. London Spe. Pub.*, **8**, 323-337.

Holland, T.J.B. (1979a): Experimental determination of the reaction paragonite = jadeite + kyanite + H_2O, and internally-consistent thermodynamic data for part of the system Na_2O-Al_2O_3-SiO_2-H_2O, with applications to eclogites and blueschists. *Contrib. Mineral. Petrol.*, **68**, 293-301.

— (1979b): High water activities in the generation of high-pressure kyanite eclogites of the Tauern Window, Austria. *J. Geol.*, **87**, 1-27.

Hughes, R.A. & Pilatasig, L.F. (2002): Cretaceous and Tertiary terrane accretion in the Cordillera Occidental of the Andes of Ecuador. *Tectonophysics*, **345**, 29-48.

Jaillard, E., Soler, P., Carlier, G., Mourier, T. (1990): Geodynamic evolution of the northern and central Andes during early to middle Mesozoic times: a Tethyan model. *J. Geol. Soc. London*, **147**, 1009-1022.

Jaillard, E., Benitez, S., Mascle, G.H. (1997): Les déformations paléogènes de la zone d'avant-arc sud-équatorienne en relation avec l'évolution géodynamique. *Bull. Soc. Géol. France*, **168**, 403-412.

Kiénast, J.-R., Lombardo, B., Biino, G., Pinardon, J.-L. (1991): Petrology of very-high-pressure eclogitic rocks from the Brossasco-Isasca Comples, dora-Maira Massif, Italian Western Alps. *J. metamorphic Geol.*, **9**, 19-34.

Konopasek, J. (2001): Eclogitic micaschists in the central part of the Krusne hory Mountains (Bohemian Massif). *Eur. J. Mineral.,* **13**, 87-100.

Koons, P.O. (1982): An investigation of experimental and natural high-pressure assemblages from the Sesia Zone, Western Alps, Italy. Dissertation, ETH Zürich, 260p.

Kretz, R. (1983): Symbols for rock-forming minerals. *Am. Mineral.*, **68**, 277-279.

Laird, J. (1988): Chlorites: metamorphic petrology. *in* "Hydrous Phyllosilicates", S.W. Bailey ed., *Mineral. Soc. Am. Reviews in Mineralogy*, **19**, 405-453.

Litherland, M., Aspden, J.A., Jemielita, R.A. (1994): The metamorphic belts of Ecuador. *Overseas Memoir British Geol. Survey*, **11**, 1-147.

Maruyama, S., Liou, J.G., Terabayashi, M. (1996): Blueschists and eclogites of the world and their exhumation. *Int. Geol. Review*, **38**, 485-594.

Massonne, H.-J. & Szpurka, X. (1997): Thermodynamic properties of white micas on the basis of high pressure experiments in the systems K_2O-MgO-Al_2O_3-SiO_2-H_2O and K_2O-FeO-Al_2O_3-SiO_2-H_2O. *Lithos*, **41**, 229-250.

Mégard, F. (1987): Cordilleran Andes ans marginal Andes: a review of Andean geology north of the Arica elbow (18°S). *in* "Circum-Pacific orogenic belts and evolution of the Pacific Ocean basin", J.W.H. Monger & J. Francheteau eds., American Geophysical Union, Geodynamics Series, **18**, 71-95.

Meyre, C., de Capitani, C., Zack, T., Frey, M. (1999): Petrology of high-pressure metapelites from the Adula Nappe (Central Alps, Switzerland). *J. Petrol.*, **40**, 199-213.

Miller, C. (1986): Alpine high-pressure metamorphism in the Eastern Alps. *Schweiz. Mineral. Petrogr. Mitt.*, **66**, 139-144.

Mourier, T., Laj, C., Mégard, F., Roperch, P., Mitouard, P., Farfan-Medrano, A. (1988): An accreted continental terrane in northwestern Peru. *Earth Planet. Sci. Lett.*, **88**, 182-192.

Orrego, L.A., Cepeda, H.V., Rodriguez, S.G.I. (1980): Esquistos glaucofanicos en el area de Jambalo, Cauca, Colombia. *Geologia Norandina*, **4**, 5-10.

Patrick, B.E. & Evans, B.W. (1989): Metamorphic evolution of the Seward Peninsula blueschist terrane. *J. Petrol.*, **30**, 531-555.

Peacock, S.M. (1996): Thermal and petrologic structure of subduction zones. *in* "Subduction: top to bottom", G.E. Bebout, D.W. Scholl, S.H. Kirby, J.P. Platt eds., *Geophysical Monograph*, **96**, 119-133.

Perchuk, L.L. (1991): Derivation of a thermodynamically consistent set of geothermometers and geobarometers for metamorphic and magmatic rocks. *in* "Progress in metamorphic and magmatic petrology. A memorial volume in honour of D.S. Korzhinskiy", L.L. Perchuk ed., Cambridge University Press, 93-111.

Pognante, U., Compagnoni, R., Gosso, G. (1980): Micro-mesostructural relationships in the continental eclogitic rocks of the Sesia-Lanzo zone (Italian Western Alps): a record of subduction cycle. *Rend. Soc. Ital. Mineral. Petrol.,* **36**, 169-186.

Powell, R. & Holland, T. (1990): Calculated mineral equilibria in the pelite system, KFMASH (K_2O-FeO-MgO-Al_2O_3-SiO_2-H_2O). *Am. Mineral.*, **75**, 367-380.

Powell, R., Holland, T., Worley, B. (1998): Calculating phase diagrams involving solid solutions via non-linear equations, with examples using Thermocalc. *J. metamorphic Geol.*, **16**, 577-588.

Rao, B.-B. & Johannes, W. (1979): Further data on the stability of staurolite + quartz and related assemblages. *N. Jb. Miner. Mh.*, **10**, 437-447.

Reynaud, C., Jaillard, É., Lapierre, H., Mamberti, M., Mascle, G.H., (1999): Oceanic plateau and island arcs of Southwestern Ecuador: their place in the geodynamic evolution of northwestern South America. *Tectonophysics*, **307**, 235-254.

Simon, G., Chopin, C., Schenk, V. (1997): Near-end-member magnesiochloritoid in prograde-zoned pyrope, Dora-Maira massif, western Alps. *Lithos*, **41**, 37-57.

Spear, F.S. (1993): Metamorphic phase equilibria and pressure-temperature-time paths. *Mineral. Soc. Am. Monograph*, 799 p.

— (1999): Real-time AFM diagrams on your Macintosh. *Geol. Materials Research*, **1(3)**, 1-18.

Spear, F.S. & Franz, G. (1986): P-T evolution of metasediments from the Eclogite Zone, south-central Tauern Window, Austria. *Lithos*, **19**, 219-234.

Spikings, R.A., Winkler, W., Seward, D., Handler, R. (2001): Along-strike variations in the thermal and tectonic response of the continental Ecuadorian Andes to the collision with heterogeneous oceanic crust. *Earth Planet. Sci. Lett.*, **186**, 57-73.

Stöckhert, B., Massonne, H.-J., Nowlan, E.U. (1997): Low differential stress during high-pressure metamorphism: The microstructural record of a metapelite from the Eclogite Zone, Tauern Window, Eastern Alps. *Lithos*, **41**, 103-118.

Thurston, S.P. (1985): Structure, petrology and metamorphic history of the Nome Group blueschist terrane, Salmon Lake area, Seward Peninsula, Alaska. *Geol. Soc. Am. Bull.*, **96**, 600-617.

Thompson, J.B. (1957): The graphical analysis of mineral assemblages in pelitic schists. *Am. Mineral.*, **42**, 842-858.

Tropper, P. & Essene, E.J. (2002): Thermobarometry in eclogites with mutiple stages of mineral growth: an example from the Sesia-Lanzo Zone (Western Alps, Italy). *Schweiz. Mineral. Petrogr. Mitt.*, **82**, 487-514.

Tropper, P., Essene, E.J., Sharp, Z.D., Hunziker, J.C. (1999): Application of K-feldspar-jadeite-quartz barometry to eclogite facies metagranites and metapelites in the Sesia Lanzo Zone (Western Alps, Italy*). J. metamorphic Geol*., **17**, 195-209.

Vidal, O., Goffé, B., Bousquet, R., Parra, T. (1999): Calibration and testing of an empirical chloritoid-chlorite Mg-Fe exchange thermometer and thermodynamic data for daphnite. *J. metamorphic Geol*., **17**, 25-39.

Vuichard, J.-P. & Ballèvre, M. (1988): Garnet-chloritoid equilibria in eclogitic pelitic rocks from the Sesia zone (Western Alps): their bearing on phase relations in high pressure metapelites. *J. metamorphic Geol*., **6**, 135-157.

Zucali M., Spalla M.I., Gosso G. (2002): Strain partitioning and fabric evolution as a correlation tool: the example of the Eclogitic Micaschists Complex int he Sesia-Lanzo Zone (Monte Mucrone – Monte Mars, Western Alps, Italy). *Schweiz. Mineral. Petrogr. Mitt*., **82**, 429-454.

Zwart, H. (1960): The chronological succession of folding and metamorphism in the central Pyrenes. *Geol. Rundsch*., **50**, 203-218.

Received 2 January 2002
Modified version received 24 January 2003
Accepted 12 June 2003